blood advances

American Society of Hematology
2021 L Street NW, Suite 900,
Washington, DC 20036
Phone: 202-776-0544 | Fax 202-776-0545
bloodadvances@hematology.org

Post-infusion PD-1+CD8+CAR-T cells identify patients responsive to CD19-CAR-T therapy in non-Hodgkin's lymphoma

Tracking no: ADV-2023-012073R2

Nathan Denlinger (Ohio State University, United States) No-Joon Song (The Ohio State University Wexner Medical Center, United States) Xiaoli Zhang (The Ohio State University, United States) Hyeongseon Jeon (The Ohio State University, United States) Chelsea Peterson (The Ohio State University, United States) Yi Wang (The Ohio State University, United States) Kelsi Reynolds (The Ohio State University, United States) Robert Bolz (The Ohio State University, United States) Jessica Miao (The Ohio State University, United States) Chunhua Song (Division of Hematology, Internal Medicine, Ohio State University, United States) Dayong Wu (The Ohio State University, United States) Wing Keung Chan (The Ohio State University, United States) Evandro Bezerra (Ohio State University, United States) Narendranath Epperla (The Ohio State University, United States) Timothy Voorhees (The Ohio State University, United States) Jonathan Brammer (The Ohio State University, United States) Adam Kittai (The Ohio State University, United States) David Bond (The Ohio State University, United States) Yazeed Sawalha (The Ohio State University, United States) Audrey Sigmund (Ohio State University Wexner Medical Center, United States) John Reneau (The Ohio State University, United States) Mark Rubinstein (The Ohio State University Wexner Medical Center, United States) Walter Hanel (The Ohio State University, United States) Beth Christian (The Ohio State University, United States) Robert Baiocchi (Ohio State University, United States) Kami Maddocks (The Ohio State University, United States) Lapo Alinari (The Ohio State University, United States) Sumithira Vasu (The Ohio State University, United States) Marcos de Lima (The Ohio State University, United States) Dongjun Chung (The Ohio State University, United States) Samantha Jaglowski (The Ohio State University, United States) Zihai Li (The Ohio State University Wexner Medical Center, United States) Xiaopei Huang (The Ohio State University, United States) Yiping Yang (The Ohio State University, United States)

Abstract:
Chimeric antigen receptor T cell therapy (CAR-T) has revolutionized treatment for relapsed/refractory (r/r) B-cell non-Hodgkin's lymphoma (NHL). Robust biomarkers and a complete understanding of CAR-T cell function in the post-infusion phase remain limited. Here we used a 37-color spectral flow cytometry panel to perform high dimensional single cell analysis of post-infusion samples in 26 patients treated with CD28 co-stimulatory domain containing commercial CAR-T (CD28-CAR-T) for NHL and focused on computationally gated CD8+ CAR-T cells. We found that the presence of post-infusion PD-1+ CD8+ CAR-T cells at the Day 14 timepoint highly correlated with the ability to achieve complete response (CR) by 6 months. Further analysis identified multiple subtypes of CD8+ PD-1+ CAR-T cells including PD-1+ TCF1+ stem-like CAR-T cells and PD-1+ TIM3+ effector-like CAR-T cells that correlated with improved clinical outcomes such as response and progression free survival. Additionally, we identified a subset of PD-1+ CD8+ CAR+ T cells with effector-like function that was increased in patients who achieved a CR and was associated with Grade 3 or higher immune effector cell-associated neurotoxicity syndrome. Here we identified robust biomarkers of response to CD28-CAR-T and highlight the importance of PD-1 positivity in CD8+ CAR-T cells post-infusion in achieving CR.

Conflict of interest: COI declared - see note

COI notes: T.J.V receives research funding from Morphosys, Incyte, Genmab, AbbVie, Recordati, Viracta, AstraZeneca and has consulted for Novartis and Recordati. A.S.K. receives research funding from AstraZeneca and Beigene, and consults for Abbvie, AstraZeneca, Beigene, Bristol-Myers Squibb, KITE a Gilead Company, Janssen, and Loxo@Lilly. D.A.B. receives research funding from Novartis, Nurix Therapeutics, Kite a Gilead Company, and Incyte and has consulted for Novartis, Nurix Therapeutics, ADC Therapeutics, and Kite a Gilead Company. Y.S. has received research funding from BMS, Celgene, TG Therapeutics, BeiGene, AbbVie, and Genmab. J.C.R receives research funding from Merck, Corvus Pharmaceuticals, Kymera Therapeutics and consults for Acrotech biopharma, Kyowa Kirin. W.H. receives research funding from Incyte. B.C. received research funding from Genentech, Acerta, Millenium and Bristol Myers Squibb. S.J. received research funding from KITE a Gilead Company, Bristol-Myers Squibb and on advisory boards for KITE a Gilead Company, Bristol-Myers Squibb, Caribou, and CRISPR. E.B. has attended advisory board meetings of Kyverna Therapeutics and Novartis.

Preprint server: No;

Author contributions and disclosures: N.D. conceptualized the project, designed and performed the experiments, collected and analyzed the data, and wrote the manuscript; N.S. performed experiments, collected and analyzed the data, and edited the manuscript; X.Z., H.J., J.M., and D.C. performed statistical analyses; C.P, Y.W., K.R., R.B, C.S., D.W., W.C., W.H., L.A., and M.P.R. assisted in performing research experiments and edited the manuscript; E.B., N.E., T.J.V., A.S.K., D.B., Y.S., A.S., J.R., W.H., B.C., R.B., K.M., L.A., S.V., M.D.L., and S.J. assisted with subject recruitment and edited the manuscript; Z.L. participated in discussion and interpretation of data, and edited the manuscript; X.H. participated in designing various parts of the study, and in discussion and interpretation of the results, and edited the manuscript; Y.Y. assisted with designing the experiments, analyzed the data, and wrote the manuscript. Z.L., X.H. and Y.Y. supervised the work.

Non-author contributions and disclosures: No;

Agreement to Share Publication-Related Data and Data Sharing Statement: For original data please contact Nathan Denlinger via email: Nathan.denlinger@osumc.edu

Clinical trial registration information (if any):

Post-infusion PD-1^{+} CD8^{+} CAR-T cells identify patients responsive to CD19-CAR-T therapy in non-Hodgkin's lymphoma

Nathan Denlinger[1, 2*], No-Joon Song[2*], Xiaoli Zhang[3], Hyeongseon Jeon[2,3], Chelsea Peterson[1], Yi Wang[2], Kelsi Reynolds[2], Robert M Bolz[1], Jessica Miao[3], Chunhua Song[1], Dayong Wu[1], Wing Keung Chan[1], Evandro Bezerra[1], Narendranath Epperla[1], Timothy J Voorhees[1], Jonathan Brammer[1], Adam S Kittai[1], David A. Bond[1], Yazeed Sawalha[1], Audrey Sigmund[1], John C Reneau[1], Mark P. Rubinstein[2], Walter Hanel[1], Beth Christian[1], Robert A Baiocchi[1], Kami Maddocks[1], Lapo Alinari[1], Sumithira Vasu[1], Marcos de Lima[1], Dongjun Chung[2,3], Samantha Jaglowski[1], Zihai Li[2,§], Xiaopei Huang[1,2,§], Yiping Yang[1,2,§].

1- Division of Hematology, Department of Internal Medicine, The Ohio State University, Columbus, OH 43210, USA
2- Pelotonia Institute for Immuno-Oncology, The Ohio State University Comprehensive Cancer Center, Columbus, OH 43210, USA
3- Department of Biomedical Informatics, The Ohio State University College of Medicine, Columbus, OH 43210, USA

*Nathan Denlinger and No-Joon Song contributed equally to this manuscript

[§]**Correspondence:**

Yiping Yang, MD, PhD**,** Division of Hematology, The Ohio State University**,** 508 Biomedical Research Tower, 460 West 12th Ave**,** Columbus, OH 43210**.** E-mail: yiping.yang2@osumc.edu
Or
Xiaopei Huang, PhD, Division of Hematology, The Ohio State University**,** 512 Biomedical Research Tower, 460 West 12th Ave**,** Columbus, OH 43210**.** E-mail: xiaopei.huang@osumc.edu
Or
Zihai Li, MD, PhD, Pelotonia Institute for Immuno-Oncology, The Ohio State University Comprehensive Cancer Center, Columbus, OH 43210. E-mail: zihai.li@osumc.edu

Short title: PD-1 Expression Post-CAR-T Correlates With Response

Word Count:
Abstract: 199
Manuscript: 3995
Tables: 1
Figures: 5
Supplemental Figures: 9
Supplemental Tables: 3
References: 42

Data sharing statement:

For original data please contact Nathan Denlinger via email: Nathan.denlinger@osumc.edu

Key Points

- After CAR-T infusion, circulating PD-1^+ CAR^+ $CD8^+$ T cells are highly associated with response to CAR-T cell therapy for Non-Hodgkin's Lymphoma.
- Spectral flow analysis reveals specific populations of stem-like and effector-like CAR-T cells which correlate with improved outcomes.

Abstract

Chimeric antigen receptor T cell therapy (CAR-T) has revolutionized treatment for relapsed/refractory (r/r) B-cell non-Hodgkin's lymphoma (NHL). Robust biomarkers and a complete understanding of CAR-T cell function in the post-infusion phase remain limited. Here we used a 37-color spectral flow cytometry panel to perform high dimensional single cell analysis of post-infusion samples in 26 patients treated with CD28 co-stimulatory domain containing commercial CAR-T (CD28-CAR-T) for NHL and focused on computationally gated $CD8^+$ CAR-T cells. We found that the presence of post-infusion $PD\text{-}1^+$ $CD8^+$ CAR-T cells at the Day 14 timepoint highly correlated with the ability to achieve complete response (CR) by 6 months. Further analysis identified multiple subtypes of $CD8^+$ $PD\text{-}1^+$ CAR-T cells including $PD\text{-}1^+$ $TCF1^+$ stem-like CAR-T cells and $PD\text{-}1^+$ $TIM3^+$ effector-like CAR-T cells that correlated with improved clinical outcomes such as response and progression free survival. Additionally, we identified a subset of $PD\text{-}1^+$ $CD8^+$ CAR^+ T cells with effector-like function that was increased in patients who achieved a CR and was associated with Grade 3 or higher immune effector cell–associated neurotoxicity syndrome. Here we identified robust biomarkers of response to CD28-CAR-T and highlight the importance of PD-1 positivity in $CD8^+$ CAR-T cells post-infusion in achieving CR.

Introduction

CAR-T cell therapy (CAR-T) directed against CD19 (CAR19) is standard of care (SOC) for patients with relapsed/refractory (R/R) B-cell non-Hodgkin's lymphoma (NHL)[1-8]. Axicabtagene ciloleucel (axi-cel) and brexucabtagene autoleucel (brexu-cel) are commercially available CAR19 products containing a CD28 co-stimulatory domain (CD28-CAR19) used to treat R/R NHL. CD28-CAR19 products historically have resulted in complete response (CR) rates of 50%-65% at 6 months, after which, disease progression is uncommon[4,8-11]. However, a significant proportion of patients still experience failure CAR19. Multiple studies have identified clinical risk factors for CAR-T failure including high disease burden, extranodal disease, poor performance status, and increased baseline inflammatory markers[12-14]. However, patients with multiple clinical risk factors can still experience success with CAR19, and patients with low risk still experience failure.

Prior studies focusing on commercial CAR-T cells have described features that correlate with clinical outcomes. More naïve-like and memory like CAR-T cells present in leukapheresis products and CAR19 infusion products have been correlated with increased response rates while increased populations of exhausted $CD8^+$ CAR-T cells correlated with worse outcomes[13,15,16]. Post-infusion peak expansion of CD28-CAR19 CAR-T cells relative to tumor burden has been correlated with improved outcomes[13], however other studies reveal a weak or no association between CAR-T expansion and outcomes[17,18].

Additionally, biomarkers to predict severe (Grade 3 or higher) immune effector cell associated neurotoxicity syndrome (ICANS) have been difficult to quantify for CD28-CAR19 products in NHL. Increased CAR-T expansion and higher baseline and peak inflammatory markers have been shown to correlate with severe ICANS in some studies, but not in others[1,10,13,19]. In acute lymphoblastic leukemia (ALL), higher pre-treatment disease burden also correlates with ICANS, but less evidence of this has been found for NHL[20]. A previous study has identified lower levels of CAR^+ Tregs post-infusion correlates with more severe ICANS[18]; however, no other features of potential direct mediators of ICANS (ex. $CD8^+$ T cells) have been found. Thus, we sought to identify more robust predictive factors identifying patients at high risk of CAR19 failure and of developing high grade ICANS in order to improve management and the clinical outcomes of patients receiving CAR-T.

In this study, we performed high-dimensional flow cytometric analysis of post-infusion $CD8^+$ CAR^+ T cell populations to identify features of patient's CAR-T cells associated with achieving CR by 6 months and who developed severe ICANS. High-dimensional analysis was performed with spectral flow cytometry, a next generation platform utilizing antibody-fluorochrome conjugates to detect a significantly increased number of surface and intracellular molecules[21]. To account for variabilities in phenotype and functionality between CAR-T cell products with different constructs and co-stimulatory domains, we focused our analysis on commercial CD28-CAR19 products used for B-cell-NHL. We found that the presence of post-infusion PD-1^+ $CD8^+$ CAR-T cells was highly associated with achievement of CR by 6 months. Further analysis identified multiple subtypes of PD-1^+ $CD8^+$ CAR-T cells that correlated with improved clinical outcomes, including PD-1^+TCF1^+ "stem-like" CAR-T cells[22-26], and PD-1^+ $TIM3^+$ effector-like CAR-T cells. Additionally, we identified a subset of $CD8^+$ CAR^+ T cells with effector-like function that was increased in patients who achieved a CR and had severe ICANS. Here we identified robust biomarkers of response and toxicity to CD28-CAR-T and highlight the importance of PD-1 positivity in $CD8^+$ CAR-T cells post-infusion in achieving CR.

Methods

Patients

Patients who received SOC axi-cel or brexu-cel for R/R NHL at the Ohio State University Comprehensive Cancer Center (OSUCCC) and who were consented to the Leukemia Tissue Bank (LTB) protocol were included in this study. Inclusion criteria: Patients with detectable CD19+ disease prior to CAR19 infusion. Exclusion criteria: Patients who had ongoing partial response (PR) which had not resolved to either CR or progressive disease (PD) at the time of final study evaluation. Patients who achieved SD as best response were included in the PD cohort. Patient samples were procured from the OSUCCC LTB after informed consent and approval by the OSU Institution Review Board (IRB) were obtained.

Samples

Patients received CD28-CAR19 from February 2022-March 2023 and had blood samples collected at time of standard of care phlebotomy at or near day 14 post-CAR-T infusion. The median day post-CAR-T of sample collection was 15.5 days for the CR cohort and 16.5 days for PD Cohort. Peripheral blood mononuclear cells (PBMC's) were isolated from fresh whole blood by density gradient centrifugation using Ficoll-Paque and cryopreserved. Healthy donor PBMC's were purchased from STEMCELL Technologies.

Clinical data were obtained retrospectively from the electronic medical record under an IRB approved protocol. Treatment response was assessed radiographically according to the Lugano criteria[27].Toxicity was evaluated by the ASTCT consensus guidelines criteria for cytokine release syndrome (CRS) and ICANS[28]. Cutoffs for lab values being defined as within normal limits(WNL) included: lactate dehydrogenase (LDH) < 190 U/L, ferritin < 322 ng/ml, and C-reactive protein (CRP) < 10 mg/L.

Spectral flow cytometry

The 37-color spectral flow cytometry panel is outlined in Supplementary Table 1. Post-infusion PBMC samples were thawed and analyzed simultaneously along with healthy donor PBMC's. Cryopreserved single-cell suspensions collected were thawed and washed with RPMI-1640 (Gibco). LIVE/DEAD fixable blue (Invitrogen) was applied to stain dead cells. Cells were washed twice with FACS buffer and the surface molecule staining antibody cocktail including Fc block was applied for 45 minutes at 4°C. After

incubation, cells were washed twice with FACS buffer and the FOXP3/Transcription factor staining buffer set (eBioscience) was applied overnight. Cells were washed twice in permeabilization buffer, and the intracellular staining antibody cocktail was added. After 2 hours of incubation at room temperature, cells were washed twice with FACS buffer; data was collected using the Aurora (Cytek) 5-laser spectral flow cytometry machine.

High-dimensional flow cytometry data analysis

Flow cytometry data was uploaded to web-based software OMIQ (https://app.omiq.ai/). Live $CD45^+$, $CD8^+$, and CAR^+ cells were gated, and UMAP (Uniform Manifold Approximation and Projection) dimension reduction and FlowSOM clustering analysis was performed. The proper number of clusters was determined using FlowSOM elbow meta-clustering analysis; FlowSOM consensus meta-clustering analysis was performed to cluster cells with unique features[29]. Characteristics of each cluster were evaluated using individual marker expressions in UMAP space and validated using clustered heatmap. For further validation, flow cytometry data was re-evaluated using FlowJo (BD) by creating 2D plots and utilizing concomitant statistical approaches. In order to quantify the amount of CAR^+ $CD8^+$ T cells present at the time of sample collection, live cell lymphocytes were gated followed by $CD45^+$ $CD3^+$ $CD4^-$ $CD8^+$ CAR^+ cells to quantify the percentage of $CD8^+$ CAR^+ T cells as a proportion of lymphocytes. This number was then multiplied by the clinically measured absolute lymphocyte count (ALC) in order to obtain the absolute number of $CD8^+CAR^+$ T cells per ul of blood.

Statistical analyses

Two-sample t-test was used for the analysis of the continuous variables and Fisher's exact test was used for the categorical variables. Normality assumption was checked prior to analysis, and majority of the variables follow normal distribution. Wilcoxon rank sum test was used to confirm our findings. The proportion of different cell types identified by flow cytometric analysis was compared using linear regression models that accounted for patient age, gender, and tumor size; the models employed the log2-transformed proportion as the response variable and the t-distribution as the reference distribution. Spearman Correlation was used to analyze correlation between cell types and clinical variables and a multivariate regression model controlling for clinical variables was used to associate cell types with

response. Kaplan-Meier analysis was used for survival outcomes, and log-rank test was utilized to evaluate statistical significance. Thresholds for separation of patient cohorts based on cell types were selected based on the optimal response separation between the groups and denoted as “high” or “low”, as was performed in previously published analyses[18]. Thus, p-values should be interpreted with caution. SAS 9.4 and R were used for all the data analyses.

Patient samples were procured from the Ohio State University (OSU) Comprehensive Cancer Center Leukemia Tissue Bank after informed consent and approval by the OSU Institution Review Board (IRB) were obtained.

Results

Patient characteristics and outcomes with commercial CD28-CAR19

Twenty-six sequential patients treated with CD28-CAR19 between February 2022 and March 2023 met inclusion criteria and had Day 14 PBMC samples analyzed simultaneously via spectral flow cytometry. Sixteen patients achieved CR by the 6-month timepoint and were included in the CR cohort. Ten patients had progression of disease within the first 6 months post-CAR-T infusion and were included in the PD cohort. Table 1 describes patient and disease characteristics and all discrete patient data analyzed are included in Supplemental File 2.

Patient and disease characteristics were for the most part well balanced between the two cohorts and were similar to those treated in real-world studies of axi-cel[9,11]. Baseline ferritin and CRP were significantly increased in the PD cohort compared to the CR cohort when analyzed as categorical variables. There were no other significant differences in clinical characteristics between the CR and PD cohorts. Toxicity, including CRS and ICANS, was not significantly different between the two cohorts (Supplemental Table 2). Progression free survival (PFS) and overall survival (OS) for the entire 26 patient cohort (Supplemental Figure 1) were similar to real-world studies with axi-cel[9,11]. Overall, our patient cohort was found to be comparable to the majority of real-world patients treated with CD28-CAR19.

Differentially abundant post-infusion $CD8^+CAR^+$ T cell clusters in CR and PD cohorts

We developed a 37-color $CD8^+$ CAR-T cell specific spectral flow cytometry panel to identify features of post-infusion $CD8^+$ CAR^+ T cells that may correlate with clinical outcomes. We targeted Day 14 samples for the analysis to ensure all patients had reached maximum expansion, as it has been shown that the range of peak expansion for CD28-CAR19 products is 5-14 days[17,30].

We first looked at the quantity of $CD8^+$ CAR^+ T cells (gating strategy shown in Supplemental Figure 2). Similar to previous reports[18], we observed no differences in the quantity of circulating CAR^+ T cells between CR and PD cohorts. This was measured as the absolute number of $CD8^+$ CAR^+ T cells (Figure 1A) and as the percent of $CD3^+$ (Supplemental Figure 3) and $CD8^+$ CAR^+ T cells in circulation (Figure 1B). However, visualization of cells through contour plots revealed areas of the UMAP in which $CD8^+CAR^+$ T cell events were more prevalent in the CR vs. PD cohort (Figure 1C). Single cell clustering

analysis resulted in 14 clusters which were mapped back to the $CD8^+$ CAR^+ T cell UMAP space (Figure 1D). Clusters 7, 8, 9, 11, 12, and 13 were found to be more abundant in the CR cohort, whereas clusters 2, 3 and 4 were more abundant in PD cohort (Figure 1E). When combined and analyzed via linear regression model, the abundance of clusters 7, 8, 9, 11, 12, and 13 was significantly higher in the CR than the PD cohort, whereas the abundance of clusters 2, 3 and 4 was significantly lower in the CR than the PD cohort (Figure 1F). These results suggest that significant qualitative differences are present within $CD8^+$ CAR^+ T cells between CR and PD cohorts.

$PD\text{-}1^+$ $CD8^+$ CAR^+ T cell clusters are increased in the CR cohort

We next examined key markers of these differentially abundant clusters in CR vs. PD cohorts. Characteristics of each cluster and individual marker expression were first evaluated by a clustered heatmap (Figure 2A). We first noted that all cell clusters increased in the CR group were $PD\text{-}1^+$, while clusters increased in the PD group were $PD\text{-}1^-$. Clusters 8 and 9, increased in the CR cohort, were $PD\text{-}1^+$ $TCF1^+$ $T\text{-}bet^-$, which is consistent with the phenotype of stem-like T cells[22-26]. These clusters also had high expression of other stem-like T cell markers such as CD28 and EOMES[22-26]. Clusters 11 and 12, increased in the CR group, were $PD\text{-}1^+$ $TIM3^+$, and expressed high levels of effector T cell markers including GZMB and T-bet. Overall, these $PD\text{-}1^+$ $TIM3^+$ $T\text{-}bet^+$ $GZMB^+$ cells had an expression pattern similar to previously described $CD8^+$ effector-like transitory T cells[22-26,31]. Clusters 7 and 13, also increased in the CR cohort, were $PD\text{-}1^+$, $TCF1^{low}$, and TOX^- with a diverse expression of EOMES and CD28 and appeared to be in transition from stem-like to effector-like transitory cells. On the other hand, clusters 2, 3 and 4, increased in the PD group, were $T\text{-}bet^+$ $GZMB^+$, but $PD\text{-}1^-$. This is in contrast with the PD-1 positivity present on $T\text{-}bet^+$ and $GZMB^+$ cells found in clusters 11 and 12 which were increased in the CR cohort. Statistical analysis revealed the CR cohort had a significantly increased population of each $PD\text{-}1^+$ $CD8^+$ CAR-T cell sub-group (Figure 2B): $PD\text{-}1^+$ $TCF1^+$ (clusters 8 & 9), $PD\text{-}1^+$ $TCF1^{low}$ TOX^- (clusters 7 & 13) and $PD\text{-}1^+$ $TIM3^+$ $T\text{-}bet^+$ $GZMB^+$ (clusters 11 & 12). The $PD\text{-}1^-$ clusters 2, 3 and 4, as shown in Figure 1, were noted to be significantly increased in the PD cohort. Comparison of UMAP dot plots depicting cellular dynamics and marker expression plots overlaid in UMAP space were used to confirm these findings (Figure 2C, D). Expression of all markers on all clusters is shown in Supplemental Figure 4A. Collectively, our data showed that at Day 14 post-CAR-T cell infusion, $PD\text{-}1^+$ CAR-T cell

groups including PD-1$^+$TCF1$^+$ stem-like T cells and PD-1$^+$ TIM3$^+$ effector-like T cells were increased in patients who achieved CR by 6 months.

Identification of key CD8$^+$ CAR$^+$ T cell types that correlate with improved clinical outcomes

To further delineate the importance of PD-1$^+$ CD8$^+$ CAR-T cell clusters in patients who achieved CR, we performed a separate analysis of spectral flow data via 2D plotting and correlated this with clinical outcomes (Figure 3; Supplemental Figure 5). Similar to dimensional reduction, 2D plot analysis again clearly identified a PD-1$^+$ TCF1$^+$ population of CD8$^+$ CAR-T cells that was more prevalent in patients who achieved a CR at 6 months (Figure 3A). A population of PD-1$^+$ TOX$^-$ EOMES$^+$ CD45RO$^+$ cells was also found to be increased in the CR cohort (Figure 3B). Additionally, the population of PD-1$^+$ TIM3$^+$ T-bet$^+$ GZMB$^+$ Tox^{low} effector-like CD8$^+$ CAR-T cells was also found to be more abundant in CR patients (Figure 3C). In the PD cohort, a PD-1$^-$ T-bet$^+$ GZMB$^+$ CD45RA$^+$ population of cells was noted to be increased (Supplemental Figure 6). This population of cells appeared to share characteristics of T cell effector memory CD45RA re-expressors (Temras)[32,33], though PD-1 was notably absent in the majority of Temras in the PD group.

We next divided patients into cohorts based on high or low percentage of each PD-1$^+$ CD8$^+$ CAR-T cell population and assessed PFS using Kaplan-Meier analysis. Three populations were analyzed: PD-1$^+$ TCF1$^+$, PD-1$^+$ TOX$^-$ EOMES$^+$ CD45RO$^+$ and PD-1$^+$ TIM3$^+$ T-bet$^+$ GZMB$^+$ CD8$^+$ CAR-T cells. We found that patients who had higher percentages of each individual population alone had significantly improved PFS (Figure 3D, E, F). We also found that the combined abundance of groupings of these cell types was significantly higher in the CR cohort (Figure 3G, H) and higher levels of these combinations of cell types correlated to increased PFS, as assessed by Kaplan-Meier analysis (Figure 3G, H). To investigate if tumor burden or baseline inflammation correlated with the presence of the PD-1$^+$, PD-1$^+$ TCF1$^+$ or PD-1$^+$ TIM3$^+$ T-bet$^+$ GZMB$^+$ CD8$^+$ CAR-T cells, we performed Spearman Correlation and multivariate regression analysis. We found no direct correlation between cell types and tumor diameter and baseline LDH. In the multivariate model (controlling for LDH, CRP, ferritin, and largest tumor diameter) we found that PD-1$^+$ CD8$^+$ CAR-T cells (though not other cell types) correlated with both patient response and tumor diameter but not baseline LDH, ferritin or CRP. When controlling for tumor burden, a higher quantity PD-1+ CD8$^+$ CAR-T cells correlated with increased chance for CR. Taken together, these results provide a basis for

quantifying easily identifiable post-infusion $CD8^+$ CAR-T cell types by 2D flow and establish associations with these cell types to improved PFS for patients treated with CD28-CAR19 in NHL.

PD-1 expression on post-infusion $CD8^+$ CAR-T cells correlates with improved clinical outcomes

Given PD-1 expression was present on all key clusters and cell types that correlated with improved clinical outcomes, we next analyzed whether PD-1 expression alone correlated with better clinical outcomes. Individual patient PD-1 expression plots revealed increased expression of PD-1 on $CD8^+$ CAR^+ T cells of patients in the CR cohort (Figure 4A). Pre- and post-infusion FDG-PET scans (Figure 4B) revealed complete responses achieved by patients with the presence of high PD-1 expression (Pt#5 and Pt#31). In comparison, PETs revealed progressive disease in patients with low PD-1 expression (Pt#6 and Pt#27). Statistical analysis of PD-1 expression on $CD8^+$ CAR^+ T cells revealed that PD-1^+ $CD8^+$ CAR^+ T cells were significantly increased in CR vs. PD (Figure 4C). Additionally, patients with a higher percentage of PD-1^+ $CD8^+$ CAR-T cells had increased PFS, as assessed by Kaplan-Meier analysis (Figure 4C). Analysis of PD-1 expression as a continuous variable revealed that for each 1% increase in PD-1^+ expression on CAR^+ $CD8^+$ cells at Day 14, the odds of achieving a CR increased by 5%. A 5% increase in PD-1^+ $CD8^+$ CAR-T cells resulted in a 28% increase in the odds of CR, and a 20% increase resulted in a 260% increase in the odds of achieving a CR. Overall, these analyses reveal that increased PD-1 expression on post-infusion $CD8^+$ CAR-T cells at Day 14 correlates with improvement in clinical outcomes.

Increased PD-1^+ $CD8^+$ CAR^+ effector-like cells correlate with severe ICANS in the CR cohort

We also evaluated toxicity to investigate for factors associated with severe (Grade 3 or higher) ICANS. The rate of any grade ICANS for the total cohort was 50% and the rate of severe ICANS was 23% (Supplemental Table 2), similar to real-world studies[9,11]. We then analyzed for features present on $CD8^+$ CAR-T cells that may have correlated with severe ICANS. Six patients had severe ICANS while 20 patients had no or non-severe ICANS (Grade 0-2). Of six patients with severe ICANS, four had CR and two had PD. Utilizing individual patient UMAPs, we found that Clusters 11 and 12 were enriched in CR patients who had severe ICANS compared to those without severe ICANS (Figure 5A). These clusters were not enriched in the two PD patients with severe ICANS (Supplemental Figure 7). We thus continued

our analysis with a focus on CR patients and ICANS. Patient and disease characteristics in CR patients were analyzed and no clinical characteristics were found to correlate with the presence of severe ICANS (Supplemental Table 3). Further analysis of baseline and peak (within 30 days post-CAR-T) inflammatory markers (LDH, ferritin, and CRP) as well as expansion of CAR-T cells at the time of sample collection revealed no correlation with severe ICANS (Supplemental Figure 8). However, linear regression analysis confirmed that Clusters 11 and 12, which were previously characterized as PD-1^{+}TIM3^{+}T-bet^{+}GZMB^{+} effector-like CD8^{+} CAR-T cells (Figure 2A), were significantly increased in patients with severe ICANS (Figure 5B). Clusters 7 and 13 were significantly increased in patients with no/non-severe ICANS while other clusters did not correlate with ICANS (Supplemental Figure 9). Subsequently, 2D flow analysis confirmed that PD-1^{+}TIM3^{+}T-bet^{+}GZMB^{+} effector-like CD8^{+} CAR-T cells were increased in the severe ICANS cohort (Figure 5C). With this analysis, we identified a CD8^{+} effector-like CAR-T cell population present at the Day 14 timepoint that correlated with severe ICANS in patients who achieved a CR.

Discussion

In this study, we found that post-infusion PD-1$^+$CD8$^+$CAR-T cells were critical for patients to achieve CR by 6 months with CD28-CAR19 for NHL. Deeper analysis identified subtypes of PD-1$^+$CD8$^+$ CAR-T cells that correlated with improved clinical outcomes, including PD-1$^+$TCF1$^+$ stem-like CAR-T cells and PD-1$^+$ TIM3$^+$ effector-like CAR-T cells. Furthermore, we identified a subset of CD8$^+$ CAR$^+$ T cells with effector-like function that was increased in the CR cohort patients who had severe ICANS.

PD-1$^+$TCF1$^+$ stem-like T cells are characterized by high proliferative capacity and the capacity for self-renewal. In models of chronic infection and cancer, they are responsible for providing a pool of functional CD8$^+$ T cells that mediate disease control and with immune checkpoint inhibitor (ICI) therapy the presence and frequency of stem-like T cells correlates with improved clinical outcomes[22-26]. To date, the presence of PD-1$^+$TCF1$^+$ stem-like CD8$^+$ CAR-T cells and their correlation to CAR-T response has not been described. Here, we clearly show that a higher frequency of stem-like CD8$^+$CAR-T cells correlated with better clinical outcomes with CD28-CAR19 for NHL. We also identified a PD-1$^+$TIM3$^+$GZMB$^+$ T-bet$^+$ Tox^{low} population of effector-like CD8$^+$ CAR-T cells which correlated with improved outcomes. These effector-like CD8$^+$ cells, as progeny of stem-like T cells, have been found to be highly proliferative and also mediate disease control[34-36].

Our study also highlights the importance of PD-1 expression on CD8$^+$ CAR$^+$ T cells post-infusion. PD-1 is often described as a marker of T-cell exhaustion; however, this is only when combined with expression of other co-inhibitory receptors (ex. TIGIT, CTLA4, TIM3). PD-1 first and foremost is a marker of T-cell activation[37]. When antigen specific T-cells encounter antigen and are adequately activated, PD-1 is upregulated[38-40]. Thus, one might expect PD-1 upregulation to be ubiquitous on CAR-T cells post-infusion, given the abundant expression of CD19 on B-cells in circulation and lymphoma cells. However, we, along with others looking at Day +7, have shown negative, low and high PD-1 expression on CAR-T cells post-infusion[17,18]. Poor PD-1 upregulation by Day 14 may denote sub-optimal activation caused by intrinsic T-cell dysfunction or other influences (i.e. systemic or tumor related immunosuppression). Here we found that neither tumor burden nor LDH correlated to less PD-1$^+$ expression and when controlling for LDH or tumor burden, PD-1$^+$ expression on CD8$^+$ CAR$^+$ T cells still associated with improved response. This suggests that the lack of PD1$^+$ upregulation may not be affected by systemic inflammation or tumor

burden but may be a T-cell intrinsic phenomenon directly related to a patient's apheresis product or final CAR-T infusion product.

Furthermore, we found that higher PD-1 expression on post-infusion $CD8^+$CAR-T cells at Day 14 correlated with improved longer-term outcomes. Prior studies have described the role of PD-1 in protecting T-cell longevity, proliferation, and optimal memory formation in stem-like T cell models of cancer, chronic infection and ICI therapy[22-26]. A knockout of PD-1 on CD8+ T-cells can lead to increased expansion, but also more rapid development of T-cell dysfunction and exhaustion, and loss of memory formation[41]. Therefore, it may be that low levels of PD-1 post-infusion result in a reduced ability for CAR-T cells to maintain and mediate ongoing response; further studies are ongoing to investigate this.

Previous studies have shown that increased tumor burden, expansion, and peak inflammation, as well as lower levels CAR^+ Tregs post-infusion correlate with more severe ICANS[1,18,20,42]. Here we found that a subset of post-infusion $CD8^+CAR^+$ T cells with the effector-like phenotype ($PD\text{-}1^+TIM3^+GZMB^+T\text{-}bet^+$) was increased in patients in the CR cohort who had severe ICANS, suggesting that these effector-like $CD8^+$ CAR-T cells may potentially play a role in the development of severe ICANS. Of note, this specific population of effector-like T cells was not prevalent in PD patients, likely because the majority of effector-like cells in PD patients lacked both PD-1 and TIM3. Further analysis with larger numbers of PD patients with severe ICANS and further studies investigating the interplay between CAR^+ Tregs, CAR-T expansion, inflammation and effector-like $CD8^+$ CAR-T cells are required.

Some limitations of our study include it's correlative, retrospective, and descriptive nature. In regard to the KM curve analysis for PFS, given there is no known biologically relevant value for the newly described cell types we had no pre-determined way to specify cutoffs for each value. Thus, cutoffs were determined post hoc, and p values and PFS based on these values should be interpreted with caution. We also did not report on $CD4^+$ CAR-T cell analyses here. Though there were some differences noted, our panel was focused on $CD8^+$ CAR-T cell phenotype and function and further studies with a focus on $CD4^+$ CAR-T cells are under way.

With this study, we highlight the importance of PD-1 positivity in $CD8^+$ CAR-T cells post-infusion, describe specific populations of post-infusion CAR-T cells, including stem-like and effector-like $CD8^+$ CAR-T cells, and investigate how $CD8^+$ CAR-T cell phenotype and function may play a role in outcomes

to CAR-T cell therapy. These results allow us to identify robust biomarkers of clinical response and toxicity to CD28-CAR19 and help further elucidate patterns of CAR-T cell population dynamics in the post-CAR-T infusion setting.

Acknowledgements

This work was funded, in part, by a Conquer Cancer - Endowed Young Investigator Award (to N.D.). N.D. was also in part supported by NIH T32 CA090223. Other sources of funding for this study included NIH grants R01 CA193167 (to Y.Y.), R01 HL151195 (to Y.Y. and X.H.), R01 CA260858 (to Y.Y. and X.H.), R01 CA262069 (to Z.L.) and P01 CA278732 (to Z.L.). This work was also supported by the OSU Leukemia Tissue Bank Shared Resource (NCI P30CA016058).

Author Contributions

N.D. conceptualized the project, designed and performed the experiments, collected and analyzed the data, and wrote the manuscript; N.S. performed experiments, collected and analyzed the data, and edited the manuscript; X.Z., H.J., J.M., and D.C. performed statistical analyses; C.P, Y.W., K.R., R.B, C.S., D.W., W.C., W.H., L.A., and M.P.R. assisted in performing research experiments and edited the manuscript; E.B., N.E., T.J.V., A.S.K., D.B., Y.S., A.S., J.R., W.H., B.C., R.B., K.M., L.A., S.V., M.D.L., and S.J. assisted with subject recruitment and edited the manuscript; Z.L. participated in discussion and interpretation of data, and edited the manuscript; X.H. participated in designing various parts of the study, and in discussion and interpretation of the results, and edited the manuscript; Y.Y. assisted with designing the experiments, analyzed the data, and wrote the manuscript. Z.L., X.H. and Y.Y. supervised the work.

Conflict of Interest Disclosures:

T.J.V receives research funding from Morphosys, Incyte, Genmab, AbbVie, Recordati, Viracta, AstraZeneca and has consulted for Novartis and Recordati. A.S.K. receives research funding from AstraZeneca and Beigene, and consults for Abbvie, AstraZeneca, Beigene, Bristol-Myers Squibb, KITE a Gilead Company, Janssen, and Loxo@Lilly. D.A.B. receives research funding from Novartis, Nurix Therapeutics, Kite a Gilead Company, and Incyte and has consulted for Novartis, Nurix Therapeutics, ADC Therapeutics, and Kite a Gilead Company. Y.S. has received research funding from BMS, Celgene, TG Therapeutics, BeiGene, AbbVie, and Genmab. J.C.R receives research funding from Merck, Corvus Pharmaceuticals, Kymera Therapeutics and consults for Acrotech biopharma, Kyowa Kirin. W.H. receives research funding from Incyte. B.C. received research funding from Genentech, Acerta, Millenium and Bristol Myers Squibb. S.J. received research funding from KITE a Gilead Company, Bristol-Myers Squibb and on advisory boards for KITE a Gilead Company, Bristol-Myers Squibb, Caribou, and CRISPR.

References

1. Neelapu SS, Locke FL, Bartlett NL, et al. Axicabtagene Ciloleucel CAR T-Cell Therapy in Refractory Large B-Cell Lymphoma. *N Engl J Med*. 2017;377(26):2531-2544.

2. Schuster SJ, Bishop MR, Tam CS, et al. Tisagenlecleucel in Adult Relapsed or Refractory Diffuse Large B-Cell Lymphoma. *N Engl J Med*. 2019;380(1):45-56.

3. Abramson JS, Palomba ML, Gordon LI, et al. Lisocabtagene maraleucel for patients with relapsed or refractory large B-cell lymphomas (TRANSCEND NHL 001): a multicentre seamless design study. *Lancet*. 2020;396(10254):839-852.

4. Locke FL, Miklos DB, Jacobson CA, et al. Axicabtagene Ciloleucel as Second-Line Therapy for Large B-Cell Lymphoma. *N Engl J Med*. 2022;386(7):640-654.

5. Kamdar M, Solomon SR, Arnason J, et al. Lisocabtagene maraleucel versus standard of care with salvage chemotherapy followed by autologous stem cell transplantation as second-line treatment in patients with relapsed or refractory large B-cell lymphoma (TRANSFORM): results from an interim analysis of an open-label, randomised, phase 3 trial. *Lancet*. 2022;399(10343):2294-2308.

6. Jacobson CA, Chavez JC, Sehgal AR, et al. Axicabtagene ciloleucel in relapsed or refractory indolent non-Hodgkin lymphoma (ZUMA-5): a single-arm, multicentre, phase 2 trial. *Lancet Oncol*. 2022;23(1):91-103.

7. Fowler NH, Dickinson M, Dreyling M, et al. Tisagenlecleucel in adult relapsed or refractory follicular lymphoma: the phase 2 ELARA trial. *Nat Med*. 2022;28(2):325-332.

8. Wang M, Munoz J, Goy A, et al. KTE-X19 CAR T-Cell Therapy in Relapsed or Refractory Mantle-Cell Lymphoma. *N Engl J Med*. 2020;382(14):1331-1342.

9. Nastoupil LJ, Jain MD, Feng L, et al. Standard-of-Care Axicabtagene Ciloleucel for Relapsed or Refractory Large B-Cell Lymphoma: Results From the US Lymphoma CAR T Consortium. *J Clin Oncol*. 2020;38(27):3119-3128.

10. Locke FL, Ghobadi A, Jacobson CA, et al. Long-term safety and activity of axicabtagene ciloleucel in refractory large B-cell lymphoma (ZUMA-1): a single-arm, multicentre, phase 1-2 trial. *Lancet Oncol*. 2019;20(1):31-42.

11. Jacobson CA, Hunter BD, Redd R, et al. Axicabtagene Ciloleucel in the Non-Trial Setting: Outcomes and Correlates of Response, Resistance, and Toxicity. *J Clin Oncol*. 2020;38(27):3095-3106.

12. Vercellino L, Di Blasi R, Kanoun S, et al. Predictive factors of early progression after CAR T-cell therapy in relapsed/refractory diffuse large B-cell lymphoma. *Blood Adv*. 2020;4(22):5607-5615.

13. Locke FL, Rossi JM, Neelapu SS, et al. Tumor burden, inflammation, and product attributes determine outcomes of axicabtagene ciloleucel in large B-cell lymphoma. *Blood Adv*. 2020;4(19):4898-4911.

14. Jain MD, Zhao H, Wang X, et al. Tumor interferon signaling and suppressive myeloid cells are associated with CAR T-cell failure in large B-cell lymphoma. *Blood*. 2021;137(19):2621-2633.

15. Deng Q, Han G, Puebla-Osorio N, et al. Characteristics of anti-CD19 CAR T cell infusion products associated with efficacy and toxicity in patients with large B cell lymphomas. *Nat Med*. 2020;26(12):1878-1887.

16. Monfrini C, Stella F, Aragona V, et al. Phenotypic Composition of Commercial Anti-CD19 CAR T Cells Affects In Vivo Expansion and Disease Response in Patients with Large B-cell Lymphoma. *Clin Cancer Res*. 2022;28(15):3378-3386.

17. Garcia-Calderon CB, Sierro-Martinez B, Garcia-Guerrero E, et al. Monitoring of kinetics and exhaustion markers of circulating CAR-T cells as early predictive factors in patients with B-cell malignancies. *Front Immunol*. 2023;14:1152498.

18. Good Z, Spiegel JY, Sahaf B, et al. Post-infusion CAR T(Reg) cells identify patients resistant to CD19-CAR therapy. *Nat Med*. 2022;28(9):1860-1871.

19. Strati P, Leslie LA, Shiraz P, et al. Axicabtagene ciloleucel (axi-cel) in combination with rituximab (Rtx) for the treatment (Tx) of refractory large B-cell lymphoma (R-LBCL): Outcomes of the phase 2 ZUMA-14 study. *Journal of Clinical Oncology*. 2022;40(16_suppl):7567-7567.

20. Santomasso BD, Park JH, Salloum D, et al. Clinical and Biological Correlates of Neurotoxicity Associated with CAR T-cell Therapy in Patients with B-cell Acute Lymphoblastic Leukemia. *Cancer Discov*. 2018;8(8):958-971.

21. Nolan JP, Condello D. Spectral flow cytometry. *Curr Protoc Cytom*. 2013;Chapter 1:1 27 21-21 27 13.

22. Siddiqui I, Schaeuble K, Chennupati V, et al. Intratumoral Tcf1(+)PD-1(+)CD8(+) T Cells with Stem-like Properties Promote Tumor Control in Response to Vaccination and Checkpoint Blockade Immunotherapy. *Immunity*. 2019;50(1):195-211 e110.

23. Escobar G, Mangani D, Anderson AC. T cell factor 1: A master regulator of the T cell response in disease. *Sci Immunol*. 2020;5(53).

24. Koh J, Kim S, Woo YD, et al. TCF1(+)PD-1(+) tumour-infiltrating lymphocytes predict a favorable response and prolonged survival after immune checkpoint inhibitor therapy for non-small-cell lung cancer. *Eur J Cancer*. 2022;174:10-20.

25. Connolly KA, Kuchroo M, Venkat A, et al. A reservoir of stem-like CD8(+) T cells in the tumor-draining lymph node preserves the ongoing antitumor immune response. *Sci Immunol*. 2021;6(64):eabg7836.

26. Yi L, Yang L. Stem-like T cells and niches: Implications in human health and disease. *Front Immunol*. 2022;13:907172.

27. Cheson BD, Fisher RI, Barrington SF, et al. Recommendations for initial evaluation, staging, and response assessment of Hodgkin and non-Hodgkin lymphoma: the Lugano classification. *J Clin Oncol*. 2014;32(27):3059-3068.

28. Lee DW, Santomasso BD, Locke FL, et al. ASTCT Consensus Grading for Cytokine Release Syndrome and Neurologic Toxicity Associated with Immune Effector Cells. *Biol Blood Marrow Transplant*. 2019;25(4):625-638.

29. Van Gassen S, Callebaut B, Van Helden MJ, et al. FlowSOM: Using self-organizing maps for visualization and interpretation of cytometry data. *Cytometry A*. 2015;87(7):636-645.

30. Locke FL, Neelapu SS, Bartlett NL, et al. Phase 1 Results of ZUMA-1: A Multicenter Study of KTE-C19 Anti-CD19 CAR T Cell Therapy in Refractory Aggressive Lymphoma. *Mol Ther*. 2017;25(1):285-295.

31. Hudson WH, Gensheimer J, Hashimoto M, et al. Proliferating Transitory T Cells with an Effector-like Transcriptional Signature Emerge from PD-1(+) Stem-like CD8(+) T Cells during Chronic Infection. *Immunity*. 2019;51(6):1043-1058 e1044.

32. Lanzavecchia A, Sallusto F. Dynamics of T lymphocyte responses: intermediates, effectors, and memory cells. *Science*. 2000;290(5489):92-97.

33. Sallusto F, Geginat J, Lanzavecchia A. Central memory and effector memory T cell subsets: function, generation, and maintenance. *Annu Rev Immunol*. 2004;22:745-763.

34. Im SJ, Hashimoto M, Gerner MY, et al. Defining CD8+ T cells that provide the proliferative burst after PD-1 therapy. *Nature*. 2016;537(7620):417-421.

35. Utzschneider DT, Charmoy M, Chennupati V, et al. T Cell Factor 1-Expressing Memory-like CD8(+) T Cells Sustain the Immune Response to Chronic Viral Infections. *Immunity*. 2016;45(2):415-427.

36. Wu T, Ji Y, Moseman EA, et al. The TCF1-Bcl6 axis counteracts type I interferon to repress exhaustion and maintain T cell stemness. *Sci Immunol*. 2016;1(6).

37. Sharpe AH, Pauken KE. The diverse functions of the PD1 inhibitory pathway. *Nat Rev Immunol*. 2018;18(3):153-167.

38. Agata Y, Kawasaki A, Nishimura H, et al. Expression of the PD-1 antigen on the surface of stimulated mouse T and B lymphocytes. *Int Immunol*. 1996;8(5):765-772.

39. Chikuma S, Terawaki S, Hayashi T, et al. PD-1-mediated suppression of IL-2 production induces CD8+ T cell anergy in vivo. *J Immunol*. 2009;182(11):6682-6689.

40. Youngblood B, Oestreich KJ, Ha SJ, et al. Chronic virus infection enforces demethylation of the locus that encodes PD-1 in antigen-specific CD8(+) T cells. *Immunity*. 2011;35(3):400-412.

41. Pauken KE, Godec J, Odorizzi PM, et al. The PD-1 Pathway Regulates Development and Function of Memory CD8(+) T Cells following Respiratory Viral Infection. *Cell Rep*. 2020;31(13):107827.

42. Strati P, Nastoupil LJ, Westin J, et al. Clinical and radiologic correlates of neurotoxicity after axicabtagene ciloleucel in large B-cell lymphoma. *Blood Adv*. 2020;4(16):3943-3951.

Editable Tables

Denlinger et al.

Title: Post-infusion PD-1$^+$ CD8$^+$ CAR-T cells identify patients responsive to CD19-CAR-T therapy in non-Hodgkin's lymphoma

Table 1: Patient and Disease Characteristics

Characteristics	Total	CR; n = 16 (%)	PD; n = 10 (%)	p
Age at Infusion	55 ± 11	55 ± 9	54 ± 14	0.81
Gender				
Female	9	5 (31.25)	4 (40.00)	0.69
Male	21	11 (68.75)	10 (60.00)	
Race/Ethnicity				NA
Caucasian	26	16 (100.00)	10 (100.00)	

ECOG PS at Baseline, n (%)				
0	13	9 (56.25)	4 (40.00)	0.40
1	12	7 (43.75)	5 (50.00)	
2	1	0 (0)	1 (10.00)	
Disease Type, n (%)				
DLBCL	16	9 (56.25)	7 (70.00)	0.54
HGBCL	3	1 (6.25)	2 (20.00)	
PMBCL	2	1 (6.25)	1 (10.00)	
Richter's	1	1 (6.25)	0 (0.00)	
MCL	1	1 (6.25)	0 (0.00)	
FL	3	3 (18.75)	0 (0.00)	
Infusion product, n (%)				
Yescarta	25	15 (93.75)	10 (100.00)	1
Tecartus	1	1 (6.25)	0 (0)	
Primary Refractory, n (%)				
No	15	11 (73.33)	4 (40.00)	0.12
Yes	10	4(26.67)	6 (60.00)	
MYC+ FISH, n (%)				
No	19	13 (86.67)	6 (60.00)	0.18
Yes	6	2 (13.33)	4 (40.00)	
Double HIT Fish, n (%)				
No	20	14 (93.33)	6 (60.00)	0.07
Yes	5	1 (6.67)	4 (40.00)	
IPI at Infusion (median)	2	2	2	1
IPI at Infusion >= 3, n (%)				
No	19	13 (81.25)	6 (60.00)	0.37
Yes	7	3 (18.75)	4 (40.00)	
Ann Arbor Stage, n (%)				
I/II	8	7 (33.75)	1 (10.00)	0.20
III/IV	18	9 (56.25)	9 (90.00)	
2nd line or 3rd line or > CART, n (%)				
2nd	3	1 (6.25)	2 (20.00)	0.54
3rd or >	23	15 (93.75)	8 (80.00)	
Bridging Therapy Chemo, n (%)				
No	13	8 (50.00)	5 (50.00)	1
Yes	13	8 (50.00)	5 (50.00)	
Bridging Therapy, n (%)				
RT only	1	0 (0)	1 (16.67)	0.43
Systemic only	13	8 (100.00)	5 (83.33)	
Dexamethasone Prophylaxis, n (%)				
No	12	7 (43.75)	5 (50.00)	1
Yes	14	9 (56.25)	5 (50.00)	
Characteristics	**Total**	**CR; n = 16 (%)**	**PD; n = 10 (%)**	**p**
Largest Tumor Diameter				0.05
Mean cm (range)	5.77 (1.0-20.0)	4.13 (1.1 – 10.0)	8.41 (1.0 – 20.0)	
Bulky > 5 cm, n (%)				
Yes	10	4 (25.00)	6 (60.00)	0.11
No	16	12 (75.00)	4 (40.00)	
Bulky > 7 cm, n (%)				0.07
Yes	7	2 (12.50)	5 (50.00)	

No	19	14 (87.5)	5 (50.00)	
Bulky > 10 cm, n (%)				
Yes	6	2 (12.5)	4 (40.00)	0.16
No	20	14 (87.5)	6 (60.00)	
SUVmax (mean ± STD)	18.65 ± 10.94	14.97 ± 8.34	23.90 ± 12.64	0.10
Disease Response on Pre-Infusion Imaging, n (%)				
PD	13	9 (56.25)	4 (40.00)	
PR	8	4 (25.00)	4 (40.00)	0.83
SD	1	1 (6.25)	0 (0.00)	
SD/Mixed	2	1 (6.25)	1 (10.00)	
N/A	2	1 (6.25)	1 (10.00)	
Circulating Disease Prior, n (%)				
Yes	3	2 (13.33)	1 (11.11)	1
No	21	13 (86.67)	8 (88.89)	
Extra-nodal Disease # of Sites, n (%)				
0	11	8 (50.00)	3 (30.00)	
1	11	6 (37.50)	5 (50.00)	0.64
2	3	2 (12.50)	1 (10.00)	
3	1	0 (0.00)	1 (10.00)	
LDH at Cell Infusion - U/L (mean ± STD)	288 ± 487	189 ± 32	445 ± 78	0.20
LDH > 190 U/L (ULN), n (%)				
No	11	7 (43.75)	4 (40.00)	1
Yes	15	9 (56.25)	6 (60.00)	
Ferritin at Cell Infusion - ng/ml (mean ± STD)	456 ± 394	314 ± 202	684 ± 519	0.02
Ferritin > wnl, n (%)				
No	16	13 (81.25)	3 (30.00)	0.02
Yes	10	3 (18.75)	7 (70.00)	
CRP at Cell Infusion – mg/L (mean ± STD	30 ± 44	19 ± 27	48 ± 60	0.10
CRP > wnl, n (%)				
Yes	10	3 (18.75)	7 (70.00)	0.02
No	16	13 (81.25)	3 (30.00)	

*ULN – Upper Limit of Normal (based on institutional parameters)

*p value <= 0.05 considered significant

Supplemental Table 1: CD8 CAR19 Specific Spectral Flow Panel

Marker	Fluorochrome	Brand	Category Number	Clone
Viability dye	Live Dead Blue	Invitrogen	L34962	n/a
CD45	BV510	BioLegend	368526	2D1
CD3	BV570	BioLegend	300436	UCHT1
CD8	Super bright	eBiosciences	62-0086-42	OKT-8

	436			
CD4	APC Fire 810	BioLegend	344662	SK3
FOXP3 (ICS)	eFluor 450	eBiosciences	48-4776-42	PCH101
CD11b	BUV661	BD Biosciences	612977	M1/70
CD56	BV750	BioLegend	362556	NCAM
CD45RA	AF532	eBiosciences	58-0458-42	HI100
CD45RO	BUV563	BD Biosciences	748369	UCHL1
ICOS	BV605	BioLegend	313538	C398.4A
PD1	BUV737	BD Biosciences	612791	EH12.1
Tim3	BV711	BD Biosciences	565566	7D3
TOX (ICS)	APC	Miltenyi	130-118-335	REA473
TCF1 (ICS)	PE	BioLegend	655208	7F11A10
CD62L	BV421	BD Biosciences	563862	DREG-56
CTLA4 (ICS)	PEDAZZLE 594	BioLegend	369616	BNI3
Lag-3	PEcy5	eBiosciences	15-2239-42	3DS223H
CX3CR1	PE-Cy7	BioLegend	341612	2A9-1
T-bet (ICS)	BV786	BD Biosciences	564141	O4-46
Ki-67 (ICS)	BUV395	BD Biosciences	564071	B56
GzmB (ICS)	AF700	BioLegend	372222	QA16A02
CAR19	BB515	Miltenyi	130-127-344	REA1297
CD69	BUV805	BD Biosciences	748763	FN50
NKG2D	BV480	BD Biosciences	746404	1D11
CD95	BUV615	BD Biosciences	752346	DX2
TIGIT	BV650	BD Biosciences	747840	741182
CD39	APCCy7	BioLegend	328226	A1
CD27	SPARK NIR 685	BioLegend	302856	323
CD28	BUV496	BD Biosciences	741168	CD28.2
BCL2 (ICS)	AF647	BD Biosciences	563600	Bcl2/100
EOMES (ICS)	PE-Cy5.5	eBiosciences	35-4877-42	WD1928
HELIOS	percp5.5	BioLegend	137229	22F6
CD57	FITC	BioLegend	359604	HNK-1
CXCR5	PE Fire 700	BioLegend	356954	J25D4
CD25	PE Fire 640	BioLegend	356148	M-A521
KLRG1	PE Fire 810	BioLegend	138437	2F1/KLRG1

*ICS = Intracellular stain

Supplemental Table 2: Toxicity and Clinical Outcomes

	Total	CR(n=16)	PD (n = 10)	p
Overall Survival Median OS in Days (Range)	215 (42-248)	224 (90-428)	142.5 (42-297)	
Progression Free Survival Median PFS in Days (Range)	120.5 (29-463)	153 (86-463)	72 (29-200)	
Worst CRS grade, n (%) None **Any grade**	4 (15.38) 22(84.62)	3 (18.75) 13 (81.25)	1 (10.00) 9 (90.0)	1.000
Worst CRS grade, n (%) 1 2	 15 (68.18) 7 (31.82)	(n=13) 8 (61.54) 5 (38.46)	(n=9) 7 (77.78) 2 (22.22)	0.6478
Worst ICANS grade, n (%) None Any grade	13 (50.00) 13 (50.00)	7 (43.75) 9 (56.25)	6 (60.00) 4 (40.00)	0.6882
Worst ICANS grade, n (%) 0-2 3-4	20 (76.92) 6 (23.08)	12 (75.00) 4 (25.00)	8 (80.00) 2 (20.00)	1.000

Supplemental Table 3: ICANS and Patient and Disease Characteristics

Characteristics	Total	No/Non-Severe ICANS (Grade 0-2) ; n = 12 (%)	Severe ICANS (Grade 3-4); n = 4 (%)	p
Gender Female Male	 5 11	 3 (25.0) 9 (75.0)	 2 (50.0) 2 (50.0)	0.55
ECOG PS at Baseline, n (%) 0 1	 9 7	 8 (66.7) 4 (33.3)	 1 (25.0) 3 (75.0)	0.26
Ann Arbor Stage, n (%) I/II III/IV	 7 9	 4 (33.3) 8 (66.7)	 3 (75.0) 1 (25.0)	0.31
Dexamethasone Prophylaxis, n (%) No Yes	 7 9	 5 (41.7) 7 (58.3)	 2 (50.00) 2 (50.00)	1
Largest Tumor Diameter Mean cm (range)	4.1 (1.0-10.0)	4.7 (1.5 – 10.0)	2.3 (1.0 – 3.2)	0.18
Bulky > 7 cm, n (%) Yes No	 2 14	 2 (16.7) 10 (83.3)	 0 (0) 4 (100.0)	1
Extra-nodal Disease >=2 sites, n (%) Yes No	 2 14	 2 (16.7) 10 (83.3)	 4 (100.0) 0 (0)	1
LDH at Cell Infusion - U/L (mean ± STD)	190 ± 32	190	188	0.9
LDH at Cell Infusion > 190 U/L (ULN), n (%) No Yes	 7 9	 5 (41.7) 7 (58.3)	 2 (50.00) 2 (50.00)	1
Ferritin at Cell Infusion - ng/ml (mean ± STD)	314±203	314	313	0.99
Ferritin at Cell Infusion > ULN, n (%) No Yes	 13 3	 10 (83.3) 2 (16.7)	 3 (75.0) 1 (25.0)	1
CRP at Cell Infusion – mg/L (mean ± STD	18.9 ± 26.8	22.8	7.3	0.33
CRP at Cell Infusion > ULN, n (%) Yes No	 7 9	 6 (50.0) 6 (50.0)	 3 (75.0) 1 (25.0)	0.59
Peak LDH Post-CART > ULN, n (%) Yes No	 12 4	 8 (66.7) 4 (33.3)	 4 (100.0) 0 (0)	0.45

Peak LDH Post-CART - U/L (mean ± STD)	264 ± 120	280	218	0.40
Peak Ferritin Post-CART > ULN, n (%) Yes No	9 7	7 (58.3) 5 (41.7)	2 (50.0) 2 (50.0)	1
Peak Ferritin Post-CART ng/ml (mean ± STD)	660 ± 532	622	775	0.64
Peak CRP Post-CART > ULN, n (%) Yes No	14 2	11 (91.7) 1 (8.3)	3 (75.0) 1 (25.0)	0.52
Peak CRP Post-CART – mg/L (mean ± STD)	93.3 ± 69.1	87.6	110.5	0.58
Worst Grade CRS, n (%) 0 1 2	 3 8 5	 3 (25.0) 6 (50.0) 3 (25.0)	 0 (0) 2 (50.0) 2 (50.0)	0.77

*ULN – Upper Limit of Normal (based on institutional parameters)
*p value <= 0.05 considered significant

Figure Legends

Figure 1. Differentially abundant CD8$^+$ CAR$^+$ T cell clusters in CR and PD cohorts. PBMCs from the Day 14 post-CAR-T timepoint were analyzed via spectral flow cytometry. **(A)** Representative 2D flow cytometry plot showing gating strategy for CAR19$^+$ CD8$^+$ CAR-T cells. Healthy donor samples were utilized as negative controls. Percentages of CD3$^+$ T cells as well as CAR19$^+$ CD8$^+$ T cells are indicated. **(B)** Left: Box plot of CAR19$^+$ CD8$^+$ cells as a percent of live CD45$^+$ CD3$^+$ lymphocytes in CR vs. PD cohorts; Right: Absolute # of CAR19$^+$ CD8$^+$ lymphocytes in CR vs. PD cohorts. **(C)** Contour UMAP plots of CAR19$^+$ CD8$^+$ T cells in CR vs. PD cohorts. **(D)** UMAP dot plot of CAR19$^+$ CD8$^+$ T cells from the total cohort (n=26). **(E)** UMAP of CAR19$^+$ CD8$^+$ T cells in CR vs. PD cohorts with clusters increased in CR colored blue (Clusters 7, 8, 9, 11, 12, 13) and clusters increased in PD colored red (Clusters 2, 3, 4). **(F)** Box plots showing combined clusters percentages of CAR19$^+$ CD8$^+$ Cells. Left: Combined clusters 7, 8, 9, 11, 12, and 13 in CR vs. PD. Right: Combined clusters 2, 3 and 4 in CR vs. PD. Box plots in **(B)** and **(F)** show quartiles with bands at the median; whiskers indicate 1.5 interquartile range; all observations overlaid as dots. P values are from linear regression analysis. $p < 0.05$ = *; $p < 0.01$ = **; $p < 0.001$ = ***.

Figure 2. PD-1$^+$ CD8$^+$ CAR$^+$ T cell clusters are increased in the CR cohort. (A) Clustered heatmap showing key marker expressions on differentially abundant CAR$^+$ CD8$^+$ clusters. Clusters 8 and 9: PD-1$^+$

TCF1^{+}. Clusters 7 and 13: PD-1^{+} TCF1^{low} TOX^{-}. Clusters 11 and 12: PD-1^{+} TIM3^{+} T-bet^{+} GZMB^{+}. Clusters 2, 3 and 4: PD-1^{-} T-bet^{+} GZMB^{+}. Color scale was determined by median normalization of each individual marker with blue representing low expression, white representing median expression and red representing high expression. **(B)** Box plots of clusters in CR vs. PD cohorts. Cluster abundance was reported as a percentage of CAR^{+} CD8^{+} T cells. **(C)** UMAP of CAR^{+}CD8^{+} T cells in CR vs. PD cohorts, colored by cluster. **(D)** Expression plots of phenotypical and functional markers present on CAR^{+} CD8^{+} T cells. Expression of markers on individual cells were overlaid onto the UMAP space in CR (top) vs. PD (bottom) cohorts. Box plots show quartiles with bands at the median; whiskers indicate 1.5 interquartile range; all observations overlaid as dots. P values are from linear regression analysis. $p < 0.05$ = *; $p < 0.01$ = **; $p < 0.001$ = ***.

Figure 3. Key post-infusion PD-1^{+} CAR^{+} CD8^{+} T cell populations correlate with clinical outcomes. 2D flow plot analysis was performed on spectral flow cytometry data from Day 14 post-CAR-T samples. **(A)** Representative 2D flow cytometry plots showing individual patient PD-1 and TCF1 expression in CAR^{+} CD8^{+} T cells and corresponding box plot quantification in CR vs. PD cohorts. **(B)** Representative 2D flow cytometry plots showing individual patient EOMES and CD45RO expression in CAR^{+} CD8^{+} PD-1^{+} TOX^{-} T cells and corresponding box plot quantification in CR vs. PD cohorts. **(C)** Representative 2D flow cytometry plots showing individual patient PD-1 and TIM3 expression in CAR^{+} CD8^{+} T-bet+ GZMB+ T cells and corresponding box plot quantification in CR vs. PD cohorts. **(D, E, F)** Kaplan-Meier (KM) analysis was used to generate PFS curves stratified by high vs. low percent of CD8^{+} CAR-T cell populations. **(D)** KM analysis of PFS for patients with high (>4%) or low (<4%) percent of this cell type; high group n=6; low group n=20. **(E)** KM analysis of PFS for patients with high (>4.7%) or low (<4.7%) percent of this cell type; high group n=13; low group n=13. **(F)** KM analysis of PFS for patients with high (>12%) or low (<12%) percent of this cell type; high group n=17; low group n=9. **(G)** Left: Box plot of the combination of PD-1^{+} TCF1^{+} cells and PD-1^{+} TIM3^{+} T-bet^{+} GZMB^{+} cells in CR vs. PD. Right: KM analysis of PFS for patients with high (>24%) or low (<24%) percent of this combination of cell types; high group n=13; low group n=13. **(H)** Left: Box plot of the combination of PD-1^{+} TCF1^{+} cells, PD-1^{+} TOX^{-} EOMES^{+} CD45RO^{+} cells, and PD-1^{+} TIM3^{+} T-bet^{+} GZMB^{+} cells in CR vs. PD. Right: KM analysis of PFS for patients with high (>25%) or low (<25%) percent of this combination of cell types; high group n=15; low group

n=11**.** For all KM curves, the x-axis was time in days from date of CAR-T infusion. Dotted lines on box plots indicate separation lines between high and low percentages of CAR-T cells in each population and were selected based on optimal response separation between cohorts. Because clinical outcomes were known during patient stratification, *p* values need to be interpreted with caution. Box plots in (**A), (B),** and **(C)** show quartiles with bands at the median; whiskers indicate 1.5 interquartile range; all observations overlaid as dots. P values are from linear regression analysis (cell type % changes) and log-rank tests (PFS). $p < 0.05$ = *; $p < 0.01$ = **; $p < 0.001$ = ***.

Figure 4. PD-1 expression on post-infusion CD8$^+$ CAR-T cells correlates with improved clinical outcomes. (A) Individual patient PD-1 expression on CAR$^+$ CD8$^+$ T cells was plotted in the UMAP space; CR (top) vs. PD (bottom). **(B)** Individual patient pre- and post-CAR-T infusion FDG-PET scans. Pre-infusion PETs were performed within 30 days of CAR-T infusion; red arrows point to site of pre-infusion lymphoma lesions. Post-infusion PETs were performed 30-60 days post-CAR-T; red arrows point to areas of resolution or progression of lymphoma. **(C)** Top: Representative 2D flow cytometry plot showing PD-1 expression in CR vs. PD cohorts. Bottom left: Box plot showing percentages of PD-1$^+$ CAR$^+$ CD8$^+$ T cells in CR vs. PD cohorts. Bottom Right: KM analysis of PFS for patients with high (>57.5%) or low (<57.5%) percent of PD-1$^+$ CD8$^+$ CAR-T cells; high group n=12; low group n=14**.** X-axis is time in days from date of CAR-T infusion. Dotted lines on box plots indicate separation lines between high and low percentages of CAR-T cells and were selected based on optimal response separation between cohorts. Because clinical outcomes were known during patient stratification, *p* values should to be interpreted with caution. Box plots show quartiles with bands at the median; whiskers indicate 1.5 interquartile range; all observations overlaid as dots. P values are from linear regression analysis (cell type % changes) and log-rank test (PFS). $p < 0.05$ = *; $p < 0.01$ = **; $p < 0.001$ = ***.

Figure 5. Higher quantities of PD1$^+$ TIM3$^+$ effector-like CD8$^+$ CAR-T cells correlate with severe ICANS in CR. Patients who achieved CR (n=16) were separated into a severe ICANS (Grade 3-4) cohort (n=4) and a no/non-severe ICANS (Grade 0-2) cohort (n=12). **(A)** Day 14 post-infusion PBMCs were analyzed by spectral flow cytometry and dimensional reduction. Individual patient UMAPs of CAR$^+$ CD8+

T cell clusters in ICANS (left) vs. no/non-severe ICANS cohorts (right) are shown, colored by cluster. Largest cross sectional tumor diameter prior to CAR-T infusion is listed underneath patient identifying numbers**.** Box plots in **(B)** and **(C)** compare characteristics in severe ICANS vs. no/non-severe ICANS cohorts. **(B)** Combined clusters 11 and 12, reported as a percent of CAR^+ $CD8^+$ T cells. **(C)** $PD\text{-}1^+$ $TIM3^+$ $T\text{-}bet^+$ $GZMB^+$ cells quantified by 2D flow analysis, reported as a percentage of CAR^+ $CD8^+$ Cells. Box plots show quartiles with bands at the median; whiskers indicate 1.5 interquartile range; all observations overlaid as dots. P values are from linear regression analysis. $p < 0.05$ = *; $p < 0.01$ = **; $p < 0.001$ = ***.

Figure 1

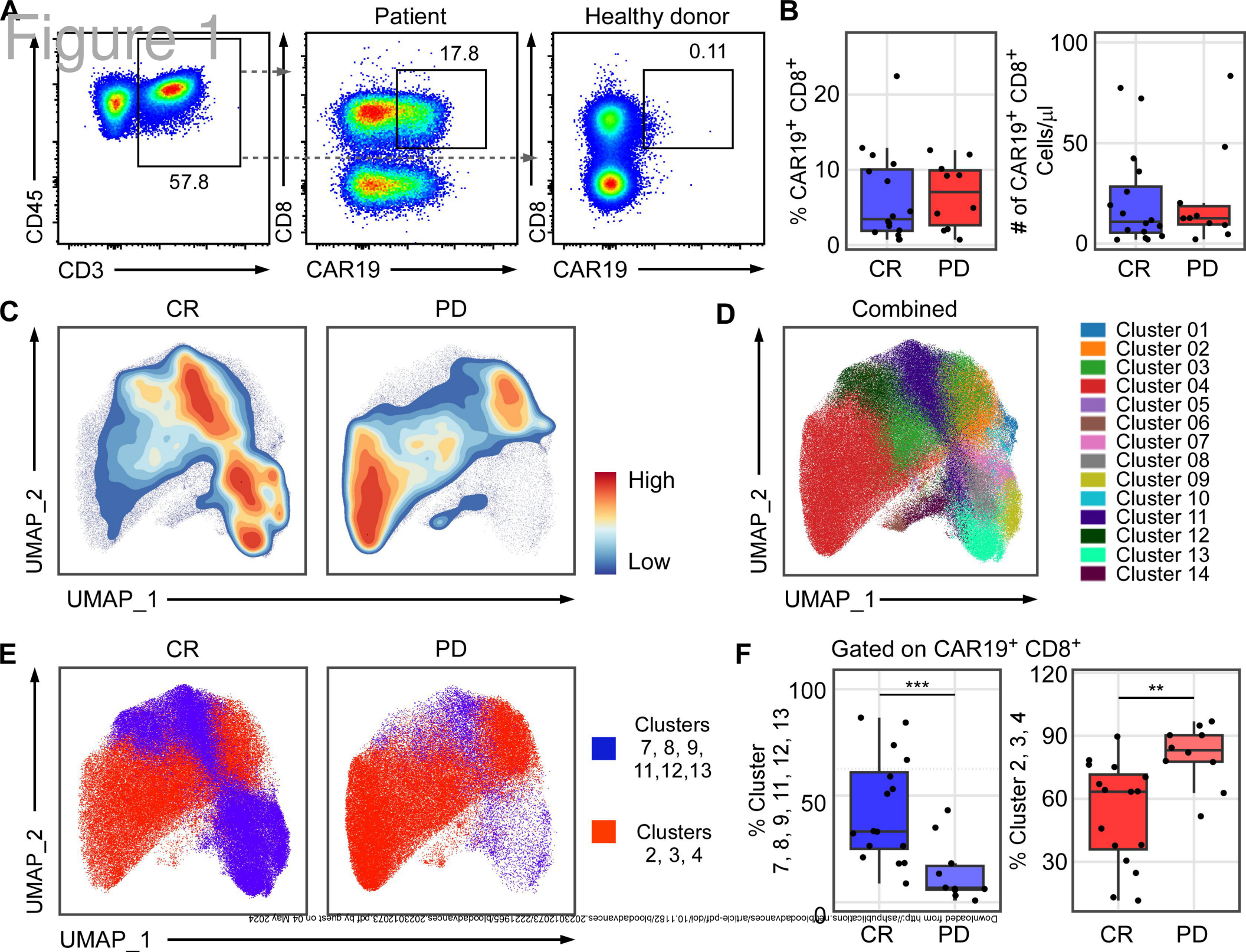

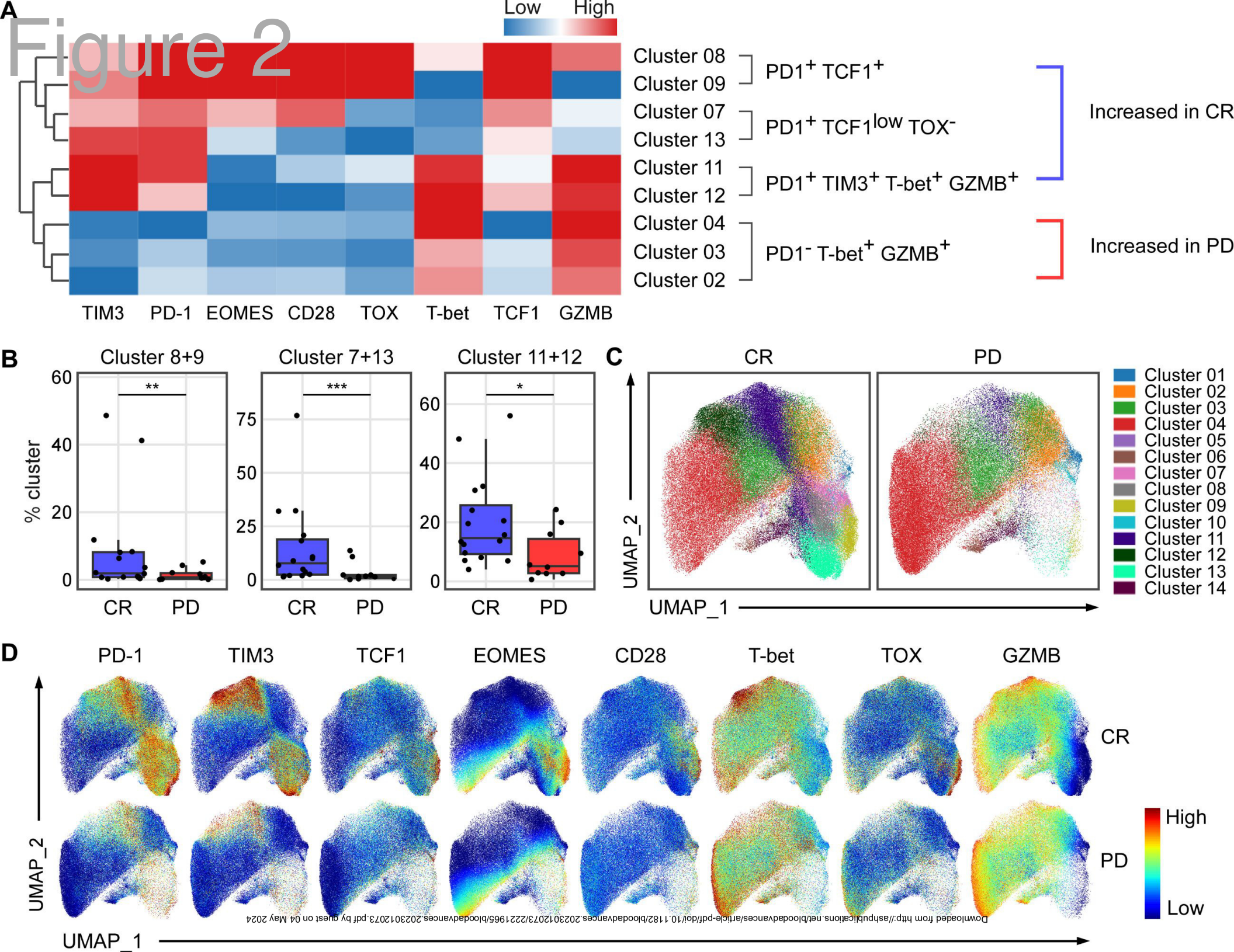

Figure 3

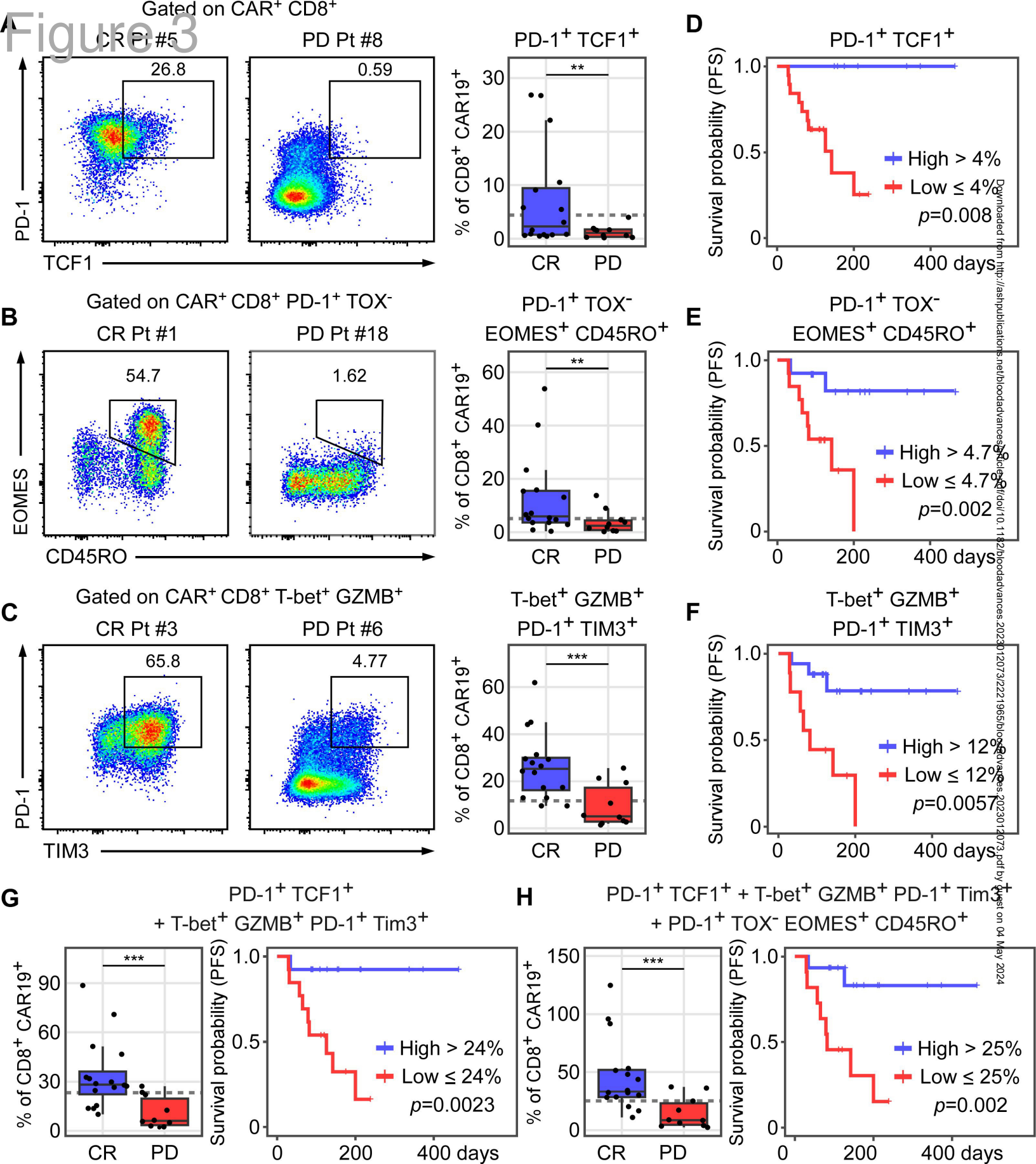

Figure 4

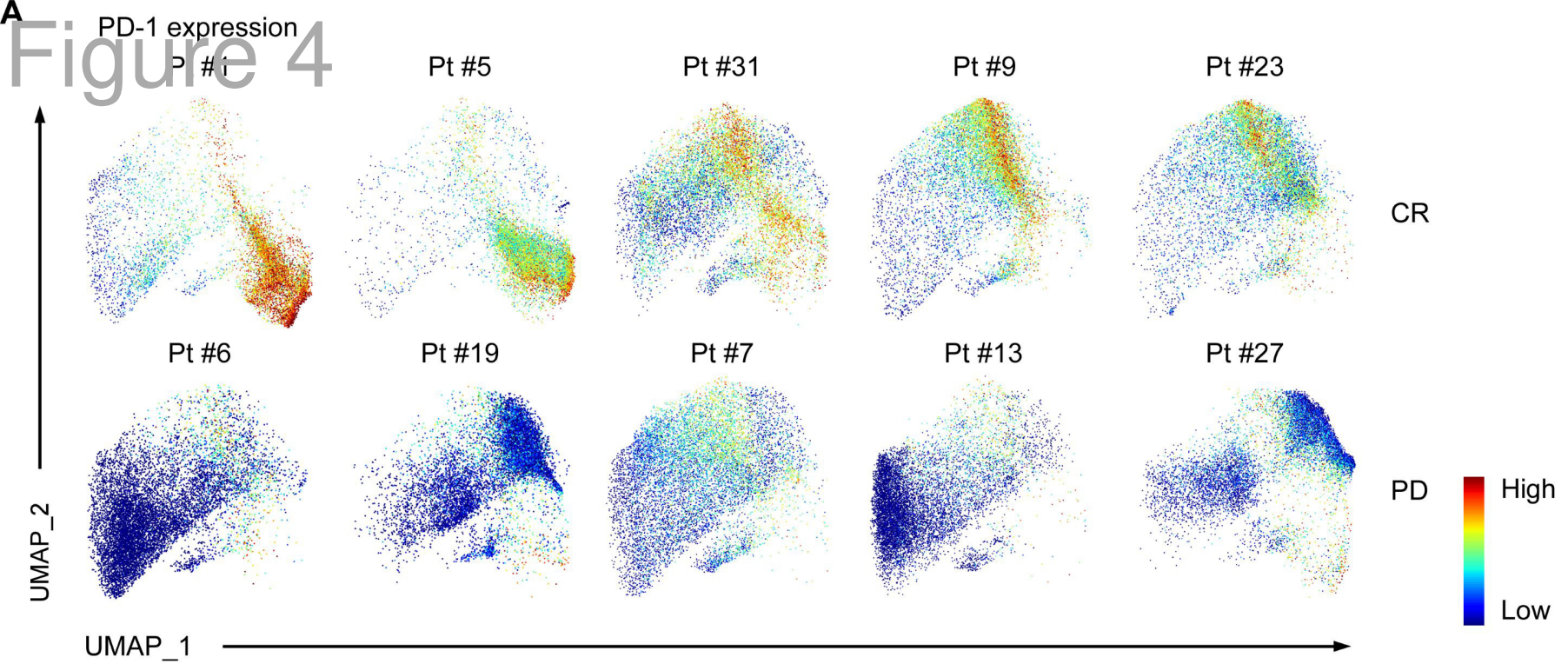

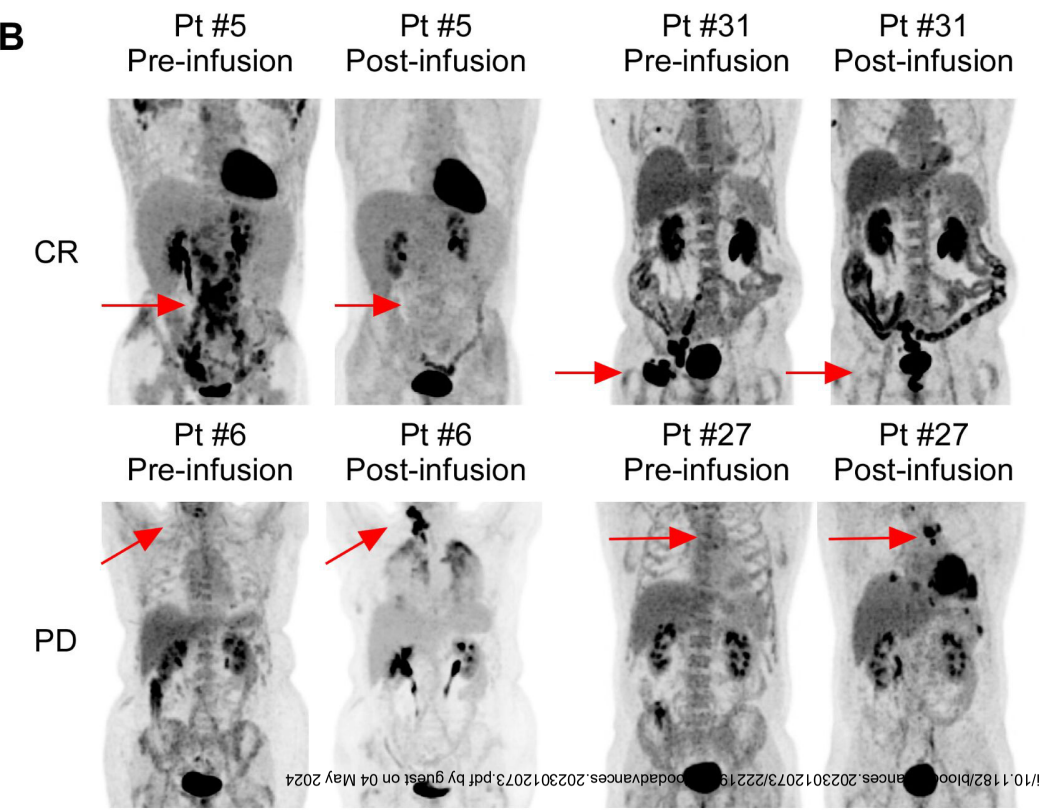

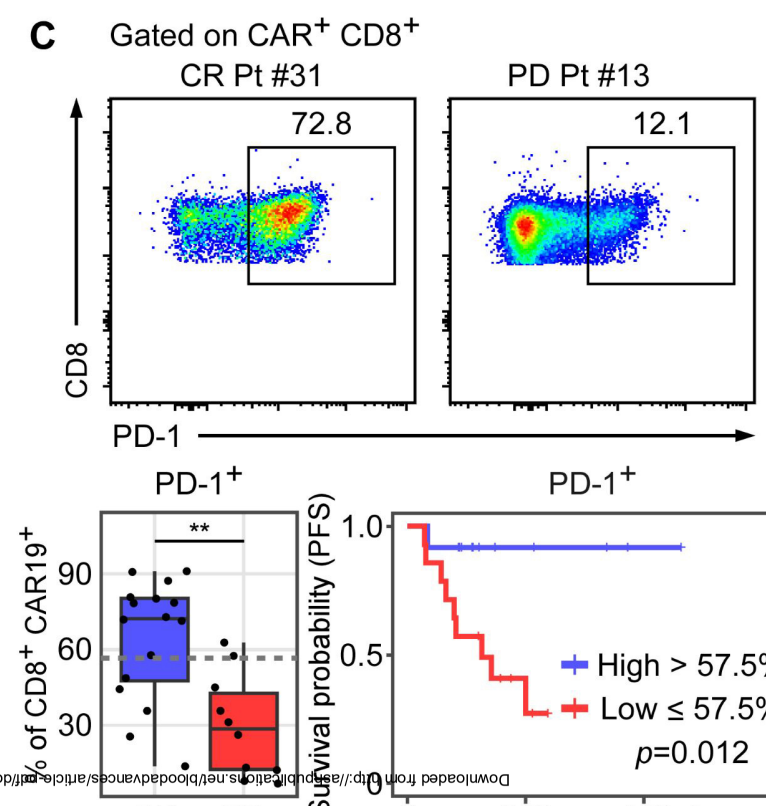

Figure 5